

Effect of γ - Irradiation on the n- Porous Silicon Structures Prepared by Electrochemical Etching

Abdulkahlig A. Sulaiman

Department of Physics/ College of Science/ University of Mosul

(Received 14 / 2 / 2018 ; Accepted 21 / 4 / 2018)

ABSTRACT

Porous Silicon has been prepared by using electrochemical cell at room temperature with etching time (20 min), current (30 mA) and fixed electrolyte solution HF:C₂H₅OH(1:4). The samples are irradiated by γ -ray with various doses (50,100) Gy. Several techniques such as scanning electron microscope (SEM), X-ray diffraction (XRD) and Raman Spectrum were used to study the influence of the γ - irradiation of porous silicon (PSi). SEM images show the random distribution of pores that cover all the surface which have different sizes and spherical shapes. XRD analysis, which indicated that n- type porous silicon and the samples irradiated at 50 and 100 Gy of γ - ray grow in hexagonal structure having preferred orientation along (002) plane in c-direction. An extremely symmetric band shape were recognized from Raman spectra of PSi.

Keywords: PSi, γ - irradiation, XRD, SEM.

تأثير تشعيع γ على تراكيب السليكون المسامي (n) المحضر بالقشط الكهروكيميائي

الملخص

حضر السليكون المسامي باستخدام الخلية الكهروكيميائية عند درجة حرارة الغرفة بزمن قشط (20 min.)، تيار (30 A) ومحلول الكتروليتي ثابت HF:C₂H₅OH(1:4). العينات تم تشعيها بأشعة γ بجرعات مختلفة (50,100 Gy). استخدمت عدة تقنيات مثل المجهر الإلكتروني الماسح (SEM)، حيود الأشعة السينية (XRD) وطيف رامان لدراسة تأثير تشعيع γ على السليكون المسامي. تبين صور SEM التوزيع العشوائي للمسامات التي تغطي جميع السطح بأحجام وأشكال دائرية مختلفة. تحليلات XRD تشير إلى أن السليكون المسامي من النوع n والعينات المشعة بأشعة γ عند (50,100 Gy) تنمو بالتركيب السداسي والاتجاه المفضل له على طول المستوي (002) بالاتجاه c. تم التعرف على شكل حزمة التناظر للسليكون المسامي إلى حد كبير من طيف رامان.

الكلمات الدالة: PSi، تشعيع γ ، XRD، SEM.

INTRODUCTION

Porous silicon is fabricated by electrochemical etching of crystalline silicon, which produces a nonporous skeleton comprised of silicon and air. The typical pore size formed in this process ranges from 5–100 nm, depending on the etching chemistry. Because the pores are smaller than the optical wavelength, porous silicon behaves like an effective medium with refractive index between that of air and silicon (Arrand *et al.*, 1998).

Complex multilayer porous structures can be fabricated by varying the current density during fabrication. Several groups have demonstrated optoelectronic devices based on porous silicon including solar cell (Arenas *et al.*, 2006), Photonic Devices (Uday, 2007), MOS detector (Alwan *et al.*, 2009), optical switches (Arenas *et al.*, 2006) and sensors (Claudia, 2013).

There is a growing interest in developing silicon photonics technology, for applications including optical interconnects, amplifiers, detectors, modulators and switches. Much of the research to date has focused on silicon on insulator ridge or channel waveguides. Porous silicon offers an interesting, although less explored, alternative to silicon on insulator structures (Paveen *et al.*, 2009).

In this study we prepared porous silicon layer by using electrochemical cell with etching time of about 20 min, current 30 mA and electrolyte solution HF:C₂H₅OH (1:4). The SEM, XRD and Raman spectrum have been used to characterized the morphology and structural properties of the samples before and after irradiation by 50 Gy and 100 Gy gamma ray.

EXPERIMENTAL

PSi is formed by an electrochemical etching of Si in an HF solution (25%). Following an electrochemical reaction occurring at the Si surface a partial dissolution of Si settles in. Let us concentrate on the various factors which rule this process. Electrolyte Usually, HF is sold in an aqueous solution with up to 25% of HF. Due to the hydrophobic character of the clean Si surface, absolute ethanol is usually added to the aqueous solution to increase the wet ability of the PSi surface. In fact, ethanoic solutions in the pores, while purely aqueous HF solutions do not. This is very important for the lateral homogeneity and the uniformity of the PSi layer in depth. In addition, during the reaction there is hydrogen evolution. Bubbles form and stick on the Si surface in pure aqueous solutions, whereas they are promptly removed if ethanol (or some other surfactant) is present. For the same reason, a careful design of the anodization cell is necessary in order to promote hydrogen bubble removal. Moreover, it has been found that lateral in homogeneity and surface roughness can be reduced. Variations in the morphology of the three PSi Figures were mainly due to the effect of the Si dissolution process, which occurred at the Si-electrolyte interface. This dissolution process was most active at the interface. There exist two types of dissolution: electrochemical and chemical. Typically, the electrochemical dissolution arises from two types of electrochemical reactions. The first is a direct electrochemical dissolution where the hydrogen-terminated Si surface is attacked by HF, thus forming unstable SiF₄ molecules. However, these unstable molecules react further with HF resulting in the more stable H₂SiF₆. The second type of dissolution is electrochemical oxidation of Si by hydroxyl ions, which leads to the formation of oxide layers. The latter is inert towards further electrochemical processes. Nevertheless, they may undergo chemical dissolution in HF solution (Suriani *et al.*, 2012).

The silicon wafer serves as the anode and it is sandwiched between the top and the bottom parts of the Teflon. The cathode is a circular gold that is submerged in the Hydrofluoric acid electrolyte, the cathode is held in place by the top part of the Teflon cell and an aluminum ring. Enough electrolyte must be present to supply the required fluorine ions and to cover the gold cathode. The top part of the Teflon cell has a circular window of area 1cm², which exposes the silicon to hydrofluoric acid and form the porous silicon. The electrochemical process is carried out under constant current 30 mA and period of about 20min. Schematic electrochemical cell shown in Fig.1.

Cs-137 radioisotope emitting 662 keV source with a dose rate of 6 Gy/min was used for exposing the samples to various irradiation doses 50 and 100 Gy, at room temperature. The Gamma-ray source was contained in a JL Shepherd Model 91-12A Irradiator.

The structure of the PSi was determined by X-ray diffraction measurements with 40 kV, 20 mA (XRD, Bruker /D8-advance with CuK α radiation ($\lambda= 1.54178 \text{ \AA}$), Germany), in the scan range of 2θ between 20°-80°- at the scanning speed of $0:02 \pm$ per second. The surface morphology of the PSi layer was investigated by scanning electron microscopy (SEM) (JEUM-JSM-6756 F) operating at a voltage of (10 keV). Then the PSi layers were characterized by using Raman spectra (GM SER No 87120, Germany).

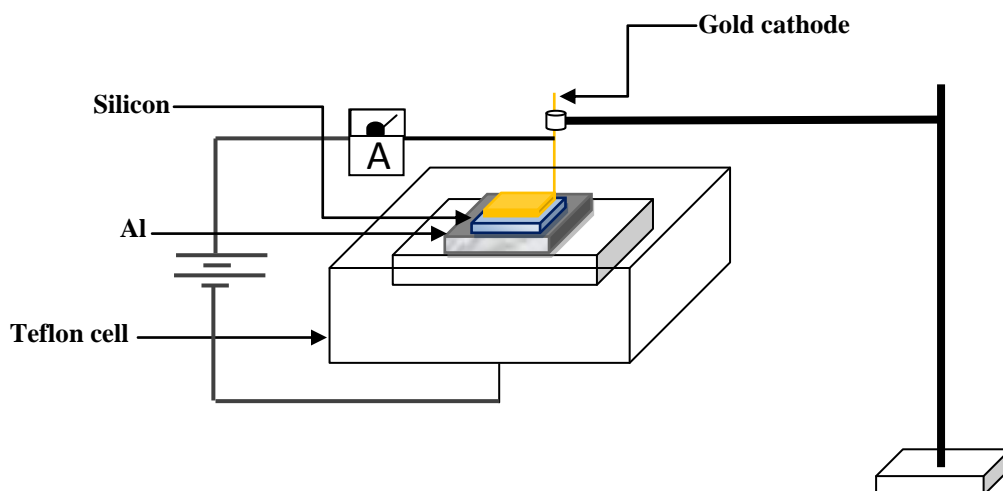


Fig. 1: Schematic electrochemical cell

RESULTS AND DISCUSSION

Structural properties:

1. Scanning electron microscopy:

Scanning electron microscopy (SEM) was used for the study of surface morphological changes of PSi prepared by electrochemical etching before and after irradiation of γ - ray.

Fig. 2 shows the surface optical microscopy image of samples a, b and c, the pores in the PSi samples are seen as dark dots. Fig. 2a shows the pores of PSi without irradiation distribute themselves randomly and are irregularly shaped. Most pores have large dimensions that seem to be joined by two or more smaller pores. The result of sample b is shown in Fig. 2b. One can see from the image that the uniformity of PSi pores has been slightly improved. The pore diameters are a larger and the shapes are more circular than in sample a. Samples b and c, were irradiated using γ - ray (50 Gy and 100 Gy) respectively.

The more irradiated dose (100 Gy) induce the more uniform distributions of homogeneous pores appear (Fig. 2c).

The uniformity obtained was attributed to the almost equal number of holes that were generated, resulting from the constant applied current density and illumination. In addition, the PSi pore diameter of sample c has been increased. The increment in pore diameter of the former case was the result of active dissolution of Si at the pore wall which enlarged the pore size, and consequently reduced the inter-pore distance. This may be due to the fast dissolution on the Si surface via a direct attack of HF followed by oxidation (Suriani *et al.*, 2012).

When gamma particles are attenuated in matter, several physical processes are active. In the general case, three interacting processes are responsible for the total attenuation: the photoelectric effect, compton scattering and pair production.

The photoelectric effect is more dominant at lower gamma ray energies ($E_\gamma < 100$ keV) and the pair production does not become significant until the gamma ray energies reach well above 3 MeV. In the intermediate energy range $E_\gamma \in [100$ keV, 3 MeV], Compton scattering is the only significant process (Jann- Rune, 1992).

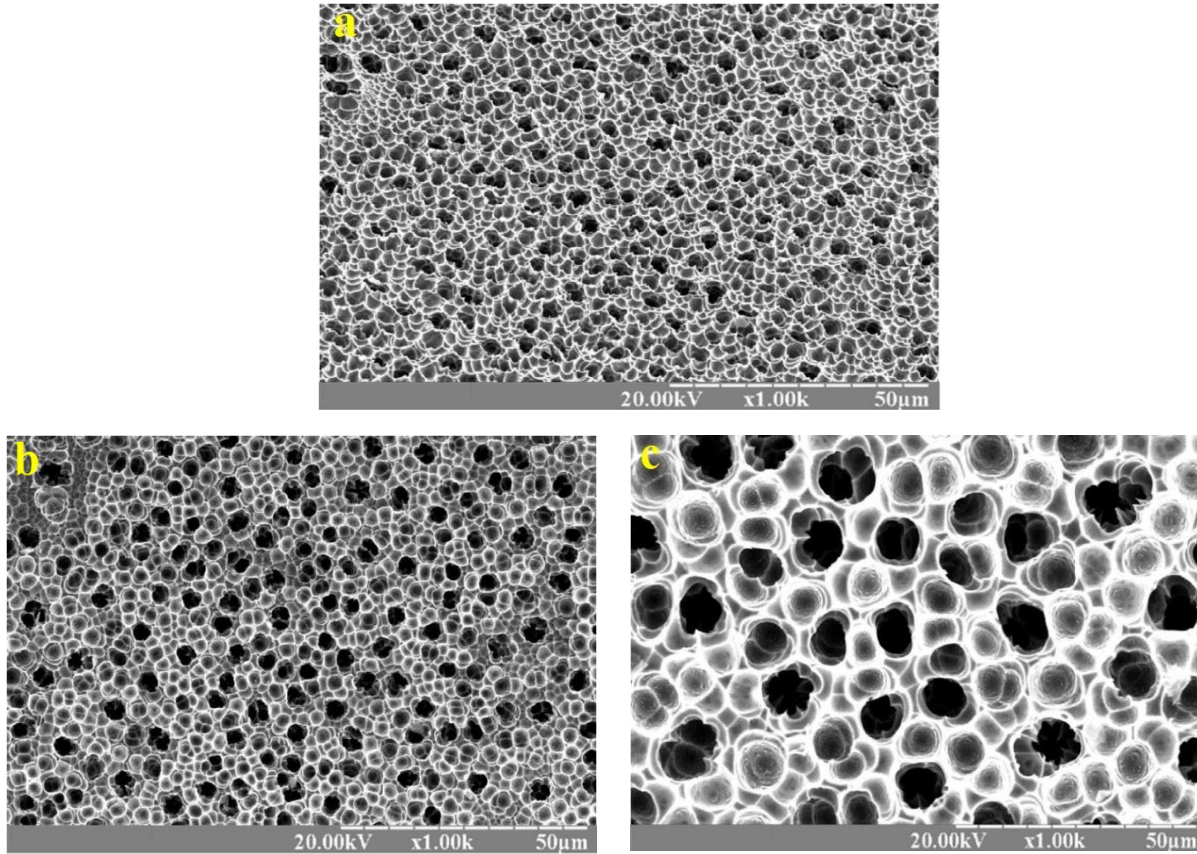


Fig. 2: SEM of PSi (a. without irradiated, b and c irradiated at 50 and 100 Gy respectively).

2. Cross-sectional SEM images:

Based on the SEM micrographs, the cross-section of the PSi layer can be divided into three distinct Figs. (a, b and c). Fig. 3 displays micrographs of the morphology of the PSi layer formed at etching time 20 s. The PSi layer without irradiation corresponds to the Fig. 3a in which the initial pores were formed within the surface of the Si substrate and the structure of the etched pores are not as good as with n-type porous silicon but the typical sizes are smaller. The main pores grew in the $\langle 002 \rangle$ direction, which was formation and morphology of highly doped n-type porous silicon perpendicular to the Si surface, as depicted in Fig. (3a). This pore growth feature persisted upon increasing the irradiation amount at 50 Gy, as shown in Fig. (3b) and we observed a cracks on the PSi surface. As the irradiation was further increased to 100 Gy, the branching structure at the surface of the bottom region of the pore disappeared, as shown in Fig. (3c). In this region, the walls were smoothed and the pores were enlarged a behavior that became more obvious at increasing the irradiation.

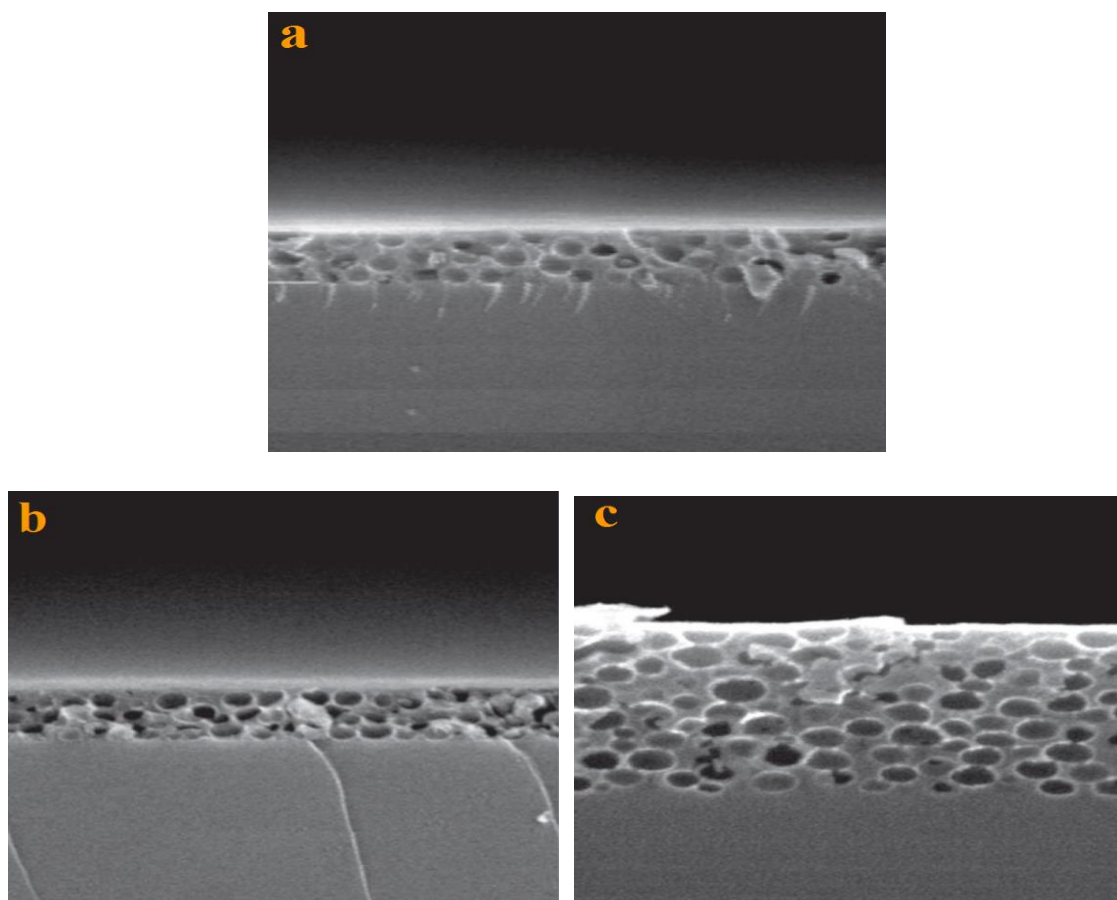


Fig. 3: Cross-sectional SEM images of PSi (a. without irradiated, b and c irradiated at 50 and 100 Gy respectively).

3. X-ray diffraction:

One important property of porous silicon is that its skeleton maintains the structure of silicon crystalline after irradiation, as shown by X-ray topography studies. The X-ray beam is diffracted at specific angular positions with respect to the incident beam depending on the phases of the sample. The X-ray diffraction pattern of PSi and irradiated PSi with γ - ray (50 and 100 Gy) with a preferred orientation of (002) is shown in Fig. (4a-c). The presence of diffraction peaks indicates the polycrystalline nature of the PSi with hexagonal (wurtzite) structure.

The X-ray diffraction peaks appearing at $2\theta = 28.5^\circ, 46.75^\circ, 55.25^\circ, 73.25^\circ$ are due to (002), (220), (311), (331) planes respectively, were observed that for PSi sample without irradiated (Fig.4a). The data are in agreement with the Joint Committee on Powder Diffraction Standards (JCPDS) card for PSi.

After irradiation with gamma ray (50 Gy), the relative intensity of distinctive (002) and other peaks (220), (311), (331) were increased, this increase in the relative intensity of each peak refers to the formation of pores that are affected by the process of irradiation as in Fig. (4b). Also we observed that the increase in the amount of irradiation (Fig. 4c) will produce a rise in the peaks intensity (002) and (220) and a decrease in the other peaks (311) and (331) with comparing to Fig. (4b), this variation in the relative intensity of the peaks can be attributed to the irradiated porous silicon surfaces at 100Gy which reduces the number of pores and this is clear from the SEM images.

When crystal size is reduced toward nanometric scale, then a broadening of diffraction peaks is observed and the width of the peak is directly correlated to the size of the nanocrystalline domains (Lorusso *et al.*, 2009). It is well known that crystallites size can be estimated from diffraction pattern analysis by measuring the full width at half maximum (FWHM) measurement and applying the Scherrer equation:

$$D = \frac{K\lambda}{\beta \cos \theta}$$

Where β is the FWHM in radians, K is the Scherrer constant equal 0.9, λ is the wavelength equal (1.54 Å), θ in radians is the diffraction angle and D the mean crystallite size (Luigi *et al.*, 2011).

The crystallites size obtained for crystalline and porous silicon samples are shown in Table (1), when estimated by the Scherrer equation, a significant crystallites size increase trend can be clearly noted on increasing γ - ray irradiation. The porous structure and the decrease of the full width at half maximum (FWHM) cause an increasing of the PSi crystallites size.

The energy bandgap of PSi layer can be calculated dependence on the size of crystals as follows (Timokhov and Timokhov, 2004):

$$E_g^* = E_g + \frac{88.34}{D^{(1.37)}}$$

Where E_g^* (eV) is the energy bandgap of PSi layer, E_g (eV) is the energy bandgap of bulk silicon and D (nm) is nanocrystallite size.

From the table (1) we shown in different irradiated doses (50 and 100 Gy) will lead to form PSi layer with smaller energy bandgap than that for PSi layer without irradiation, which is bigger than that for crystalline silicon substrate 1.12 eV (indirect, 300 K) (Sze and Ng, 2007). This is due to the increased in nanocrystallite size of PSi after irradiated with γ - ray.

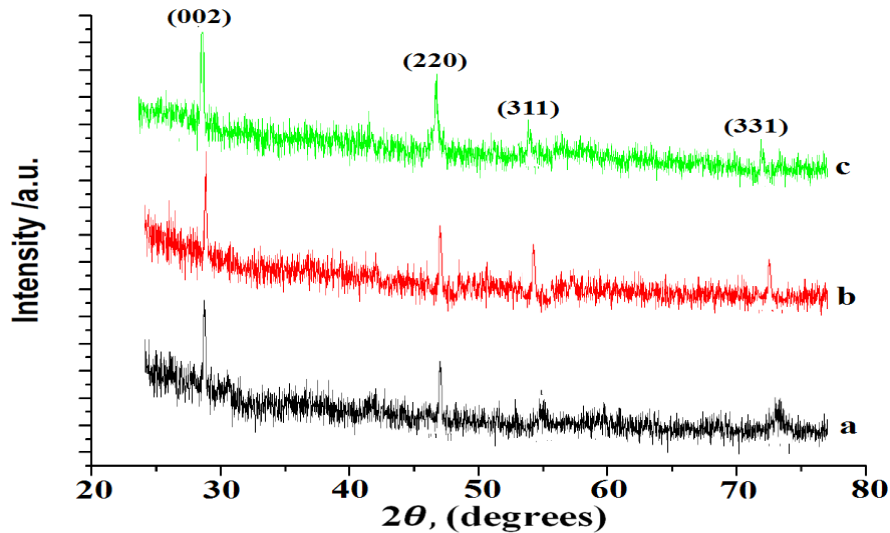


Fig. 4: XRD pattern of porous silicon (a) without irradiation, (b) after irradiation with γ - ray 50 Gy and (c) 100 Gy.

Table 1: XRD results for porous silicon before and after irradiation with γ - ray 50 and 100 Gy.

Sample (n-PSi)	hkl	2 θ (deg.)	FWHM (deg.)	D (Å°)	Eg*(eV)
a	(002)	28.5	0.5	2.86	2.01
	(220)	46.75	0.75	2.01	2.56
	(311)	55.25	0.78	2.0	2.57
	(331)	73.25	0.79	2.19	2.41
b	(002)	28.25	0.35	4.08	1.66
	(220)	46.5	0.38	3.98	1.68
	(311)	54.25	0.41	3.80	1.72
	(331)	72.5	0.45	3.82	1.72
c	(002)	27.5	0.25	5.77	1.46
	(220)	46.0	0.3	5.02	1.53
	(311)	53.75	0.28	5.56	1.47
	(331)	71.75	0.25	6.86	1.38

4. Raman Spectra:

Fig. (5) shows Raman spectrum before and after irradiation for n-type porous silicon of <002> orientation, the band shape was non symmetric for Figs. (a,b and c). This shift of the phonon peaks towards larger wave number and broadening of the peak width with increase γ -ray irradiation at 100 Gy is attributed to the confinement of optical phonon in nanodimensional PSi crystallites between the pores.

Essentially, the same Raman spectrum is seen using each of the two doses irradiation and pure PSi layer with the relative peak intensity, the structure of the PSi layer is fairly homogeneous and the phonon frequency (phonon peak shift) appears at (514 cm^{-1}) which is used to determine crystal size as in the following equation (Paillard *et al.*, 1999):

$$\Delta w = -A \left(\frac{a}{L} \right)^\gamma$$

a: Lattice constant = 0.543 Å , $A = 52.3$ and $\gamma = 1.586$: Parameters are used to describe the oscillator warming which due to finite size in the nanocrystalline.

L: crystal size = 1.92 nm .

Δw : optical phonon shift between the location of Raman band of PSi ω_{PSi} and the location of bulk Si ($\omega_{cSi} = 521 \text{ cm}^{-1}$) (Beeman *et al.*, 1985) as given in the following equation:

$$\Delta w = \omega_{PSi} - \omega_{cSi}$$

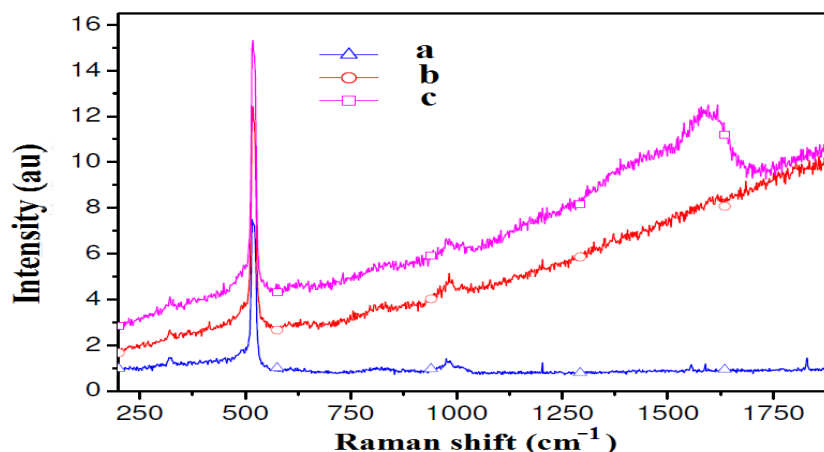


Fig. 5 : Raman spectrum (a) before irradiation, (b) after 50 Gy of γ - ray irradiation and (c) 100 Gy of γ - ray irradiation.

CONCLUSION

The influence of irradiation on the structural properties of the porous silicon prepared by electrochemical etching were investigated. XRD measurements indicate that the synthesized PSi and PSi irradiated with γ - ray are in the hexagonal phase with a preferred orientation (002). The crystallites size increase trend can be clearly noted on increasing γ - ray irradiation. The energy band gap has been decreased with the increasing irradiation doses. SEM images show that better crystalline behavior for the PSi layer by increasing irradiation. The Raman spectrum is seen using γ - irradiation at (50,100 Gy) and pure PSi layer with the relative peak intensity (514 cm^{-1}).

REFERENCES

- Alwan, M.A.; Wafaa, K.K.; Narges, Z.A. (2009). Physical Properties of MOS Porous Silicon Detector Fabricated under RTO Method. *Eng. and Tech. J.*, **27**(11), 2286- 2290.
- Arenas, M.C.; Hu, H.; Del Rio, J.A.; Snchez, A.; Nicho-Daz, M. E. (2006). Electrical properties of porous silicon/ polypyrrole heterojunctions. *Solar Energy Materials and Solar Cell.* **90**, 2413-2420.
- Arrand, H.F.; Benson, T.M.; Sewell, P.; Loni, A.; Bozeat, R.J.; Arens-Fischer, R.; Uger, M.Kr.; Onissen, M.Th.; Uth, H.L. (1998). The applications of porous silicon to optical waveguiding technology. *IEEE J. Sel. Top. Quantum Electron.*, **4**, 975–982.
- Beeman, D.; Tsu, R.; Thorpe, M.F. (1985). Structural information from the Raman Spectram of a morphous silicon. *Phys. Review B*, **32**, 874-878.
- Claudia, P. (2013). Photonic crystal sensors based on porous silicon. *Sensors*, **13**, 4694-4713.
- Jann-Rune, Ursin (1992). Detection of fluid saturation levels in porous media using gamma ray tomography. *J. Petroleum Sci. and Engi.*, **7**, 297-308.
- Lorusso; Nassisi, A.V.; Congedo, G.; Lovergine, N.; Velardi, L.; Prete, P. (2009). Pulsed plasma ion source to create Si nanocrystals in SiO₂ substrates. *J. Applied Surface Sci.*, **255**, 5401-5404.
- Paillard, V.; Puech, P.; Laguna, M. A.; Carkes, R.; Kohn, B.; Huisken, F. (1999). Improved one phonon confinement model for an accurate size determination of silicon nanocrystal. *J. Appl. Phys.*, **86** (4), 1921-1924.
- Paveen, A.; Andrea, M.; Rossi, Thomas; Murphy, E. (2009). Nonlinearities in porous silicon optical waveguides at 1550 nm. *J. Optics Express*, **17**, No. 5, 3396.
- Suriani, Y.; Mohamad, Abu Bakar ; Jamil, I.; Noor, H.H.; Kamarulazizi, I. (2012). The formation and morphology of highly doped n-type porous silicon: effect of short etching time at high current density and evidence of simultaneous chemical and electrochemical dissolutions. *J. Physical Sci.*, **23** (2), 17–31.
- Sze, S.M.; Ng, K.K. (2007). "Physics of Semiconductor Devices". 3rd Copyright Jone Wiley and Sons, Inc.
- Timokhov, D.F.; Timokhov, F.P. (2004). Determination of structure parameters of porous silicon by the photoelectric method. *J. Phys. Studies.*, **8**(2), 173-177.
- Uday, M.N. (2007). Photonic devices based on porous silicon layers. *Engi. and Technolo.*, **25**, 696-701.